J Mol Model (2010) 16:939–950
DOI 10.1007/s00894-009-0604-0

ORIGINAL PAPER

Exploration of structure, potential energy surface, and stability of planar C_3B_3

Jingling Shao · Rongwei Shi · Cheng Wang · Xiaolei Zhu · Xiaohua Lu

Received: 10 September 2009 / Accepted: 27 September 2009 / Published online: 17 October 2009
© Springer-Verlag 2009

Abstract The geometrical structures, potential energy surface, stability, and bonding character of low-energy isomers of planar C_3B_3 were systematically explored and investigated at the B3LYP/6-311+G(d)// CCSD(T)/6-311 +G(d) level for the first time. A large number of planar structures for low-energy isomers of C_3B_3 are located and reported. In particular, isomers **1** (C_s,^{2}A') and **2** (C_s,^{2}A'), with a belt-like structure corresponding to the lowest-energy structures of planar C_3B_3, are revealed. Based on molecular orbital (MO) and natural bond orbital (NBO) analyses, delocalized σ MOs, multi-centered σ MOs, and delocalized π MOs play an important role in stabilizing the structures of low-energy isomers of C_3B_3. It is interesting to note from isomerization analysis that the interconversion of isomers **2** and **7** can be realized through two isomerization channels. The results demonstrate that isomers **1**, **2**, **3**, **4**, **7**, **9**, **12**, **17**, **19**, and **20** of C_3B_3 are stable both thermodynamically and kinetically at the B3LYP/ 6-311+G(d)// CCSD(T)/ 6-311+G(d) level, and that they are observable in the laboratory, which is helpful for future experimental studies of C_3B_3.

Keywords C_3B_3 · Density functional theory · Stability · Isomerization · Potential energy surface

Electronic supplementary material The online version of this article (doi:10.1007/s00894-009-0604-0) contains supplementary material, which is available to authorized users.

J. Shao · R. Shi · C. Wang · X. Zhu (✉) · X. Lu (✉)
State Key Laboratory of Materials-Oriented Chemical Engineering, College of Chemistry and Chemical Engineering, Nanjing University of Technology,
Nanjing 210009, China
e-mail: xlzhu@njut.edu.cn
e-mail: xhlu@njut.edu.cn

Introduction

Recently, the structure, stability, and electronic properties of mixed III–V group clusters and other clusters have attracted much interest, both theoretically and experimentally [1–17].

Boron-carbon clusters have been the topic of experimental and theoretical studies [18–47]. Because boron-carbon materials, including nanowire [18, 19], nanosprings [20], and nanobelts [21, 22], exhibit resistance to high temperature and acid, and have a high degree of hardness and strength, they have many potential applications, e.g., in nuclear fission reactors [23] and spacecraft [24].

Experimentally, the structures of small boron-carbon clusters, including BC [25] and BC_2 [26], linear BC_3 and B_2C_2 [27], have been determined by electron spin resonance spectroscopy and Fourier transform infrared spectroscopy. C_nB^-(n<13) [28] and $B_{n-m}C_m$ (m≥2) [29] clusters have been obtained via direct laser vaporization and reactive molecular ion irradiation, respectively. The negative and positive C_nB_m (up to m + n = 17) cluster ions [30] generated in the laser plasma of the boron carbide target have been detected using mass spectroscopy.

Theoretically, Wang et al. [28] found that boron-terminated linear structures in C_nB^-(n<13) ions are the most stable structures at the HF/3-21G level. However, Zhan et al. [31] claimed that the lowest-energy geometries of C_nB^-(n=5–7) clusters are very floppy rather than being linear at higher theoretical levels. Pascoli and Lavendy [32] proposed that C_nB^+ cation clusters are planar monocycles based on density functional theory (DFT) methods. The geometries, electronic structures, and spectra of C_nB^q (n=1–6,q=0, ±1) clusters [33] have been studied at the B3LYP/ 6-311+G(3df) level. Belbruno and coworkers [34] studied the isomers of C_nB and C_nB_2 (n=4–10) at the B3LYP/6-311G(d,p) level, and predicted that linear and

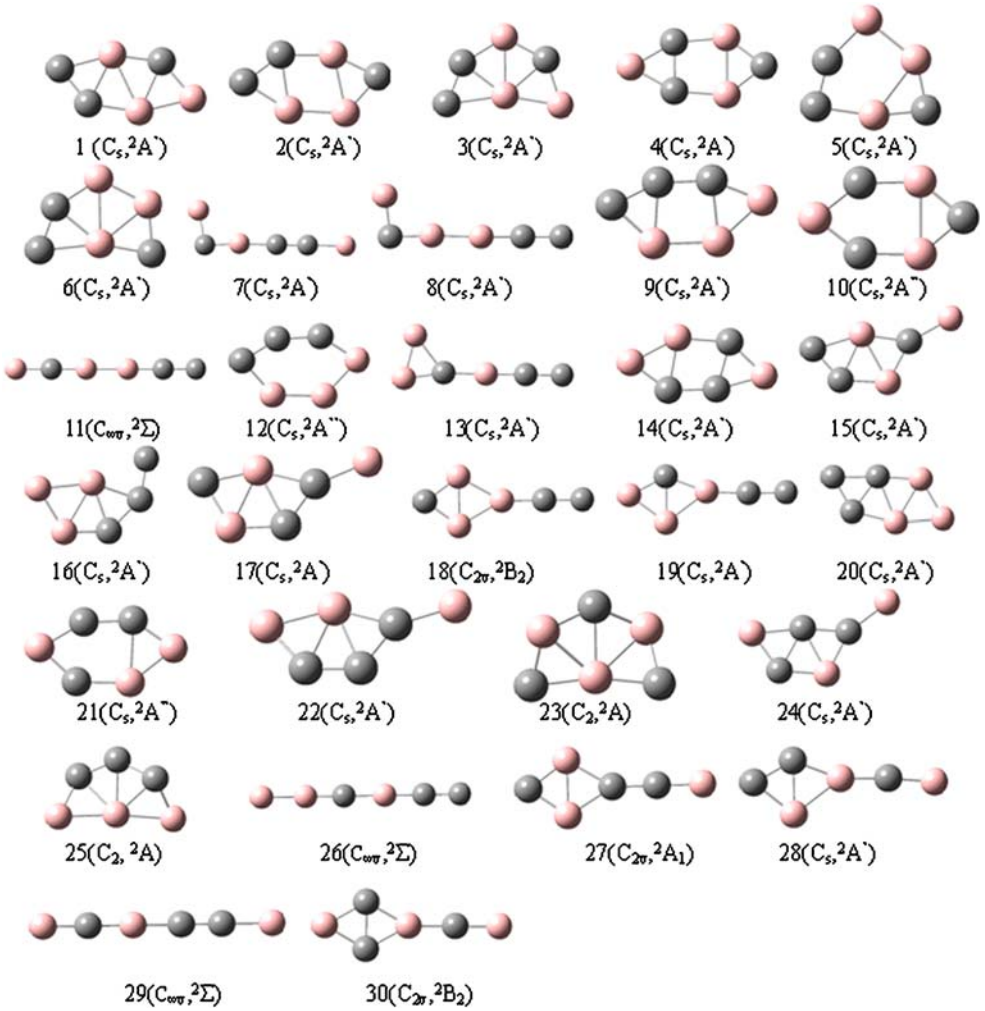

Fig. 1 Structures of low-energy isomers of planar C_3B_3 at the B3LYP/6-311+G(d) level. Point groups and electronic states are shown in parenthesis. *Gray balls* Carbon atoms, *pink balls* boron atoms

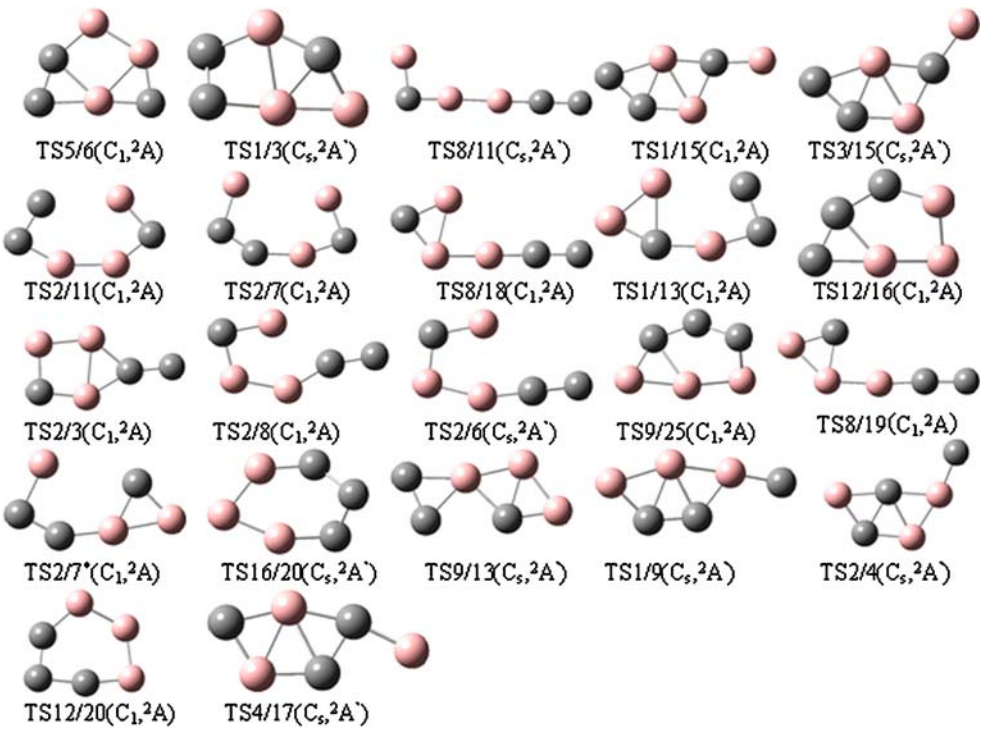

Fig. 2 Structures of transition states at the B3LYP/6-311+G(d) level. Point groups and electronic states are shown in parenthesis. *Gray balls* Carbon atoms, *pink balls* boron atoms

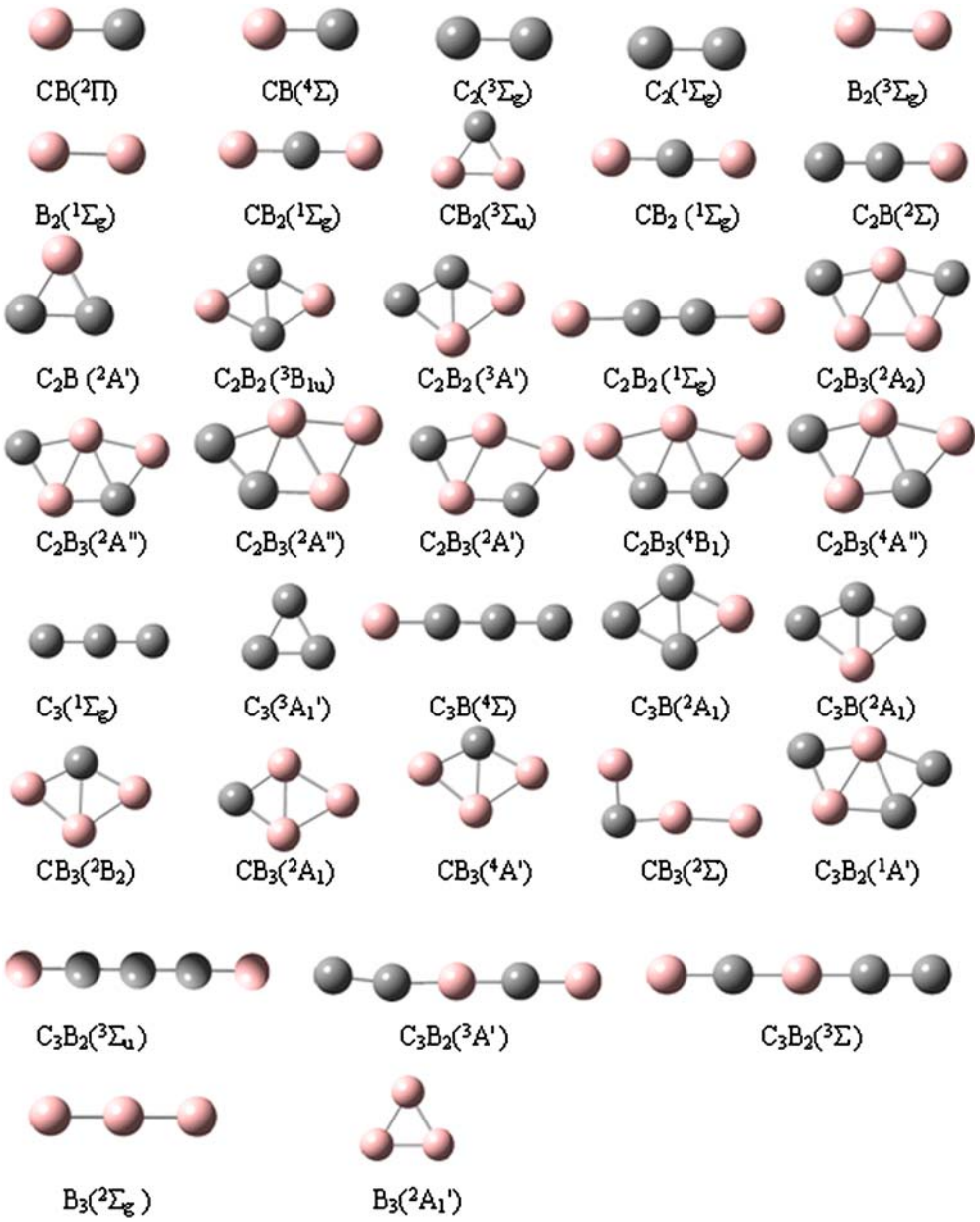

Fig. 3 Optimized fragments of the dissociations at the B3LYP/6-311+G(d) level. *Gray balls* Carbon atoms, *pink balls* boron atoms

cyclic structures coexist for $n=5$, and that cyclic structures are the exclusive form when $n\geq 6$. We previously reported that the lowest-energy structures of monocyclic C_nB_4 ($n=2$–9) clusters [35] are composed of C_m ($m=0$–2) and C_n ($n=0$–5) carbon chains by two B–C–B bridges under the constraint of C_{2v} symmetry (or D_{2h} symmetry if $m=n$).

Most of the studies cited above investigated carbon-rich boron-carbon clusters. The geometrical structures and growth patterns of boron-rich boron-carbon clusters involving B_nC ($n=1$–7) [36] and B_nC_2 ($n=1$–6) [37] have also been investigated using the B3LYP/6-311+G(d) method. Planar hypercoordinate (tetra- [38], penta [39], hexa- [40], hepta- [41], and octacoordinate [42]) carbons have been found in carbon-boron mixed clusters from theoretical calculations. Aside from the studies referred to above, the interconversion of isomers for carbon-boron binary clusters has been investigated. McAnoy et al. [43] suggested that CCBCC (**1**), with excess energy of 16.1 kcal mol^{-1}, can rearrange to planar cyclic C_4B (**19**), and that the ring of C_4B (**19**) can open to form the linear structure CCCCB (**3**) if C_4B (**19**) can overcome the energy barrier of 24.4 kcal mol^{-1}. Liu et al. reported the interconversion of various isomers of CB_4 [44], B_5C, and C_5B [45] using DFT methods. Structures with three-membered boron rings are lower in energy for isomers of B_4C and B_5C clusters, while configurations possessing three-membered carbon rings are unfavorable to the energy of C_5B.

As mentioned above, the positive and negative C_3B_3 have been detected experimentally [30]. However, there

Table 1 Relative energies (kcal mol^{-1}) of low-energy isomers of planar C_3B_3 at different levels of theory with 6-311+G(d) basis set

Isomers	B3LYP[a]	QCISD	QCISD(T)	CCSD	CCSD(T)
1[b,c]	0.0	0.0	0.0	0.0	0.0
2[b]	-0.4	0.9	0.0	1.1	0.2
3	10.1	9.4	9.6	9.2	9.4
4	17.9	15.6	16.1	16.0	16.1
5	18.3	16.1	16.8	17.3	17.6
6	18.7	19.8	19.2	20.1	19.6
7	29.5	23.4	26.5	23.3	26.4
8	23.5	26.1	25.9	26.7	26.6
9	27.1	28.6	27.4	28.8	27.6
10	31.2	32.4	28.1	33.9	28.9
11	20.0	28.7	28.6	29.8	29.7
12	38.2	40.4	36.1	41.3	36.3
13	33.6	37.1	36.6	37.8	37.8
14	41.4	41.4	41.1	41.6	41.2
15	32.1	43.0	34.4	45.4	41.5
16	44.0	42.8	42.0	43.0	42.8
17	52.2	64.9	44.5	57.5	43.5
18	38.8	42.6	43.7	44.1	44.0
19	39.8	44.6	44.5	46.0	44.5
20	47.1	46.5	45.5	46.5	45.5
21	50.0	53.3	46.3	54.2	47.2
22	52.2	47.2	48.8	46.9	48.6
23	48.5	51.8	50.1	53.4	51.1
24	55.8	50.6	52.7	50.3	52.3
25	53.6	55.7	52.8	54.2	53.2
26	42.9	54.3	49.5	54.2	55.9
27	56.0	58.8	57.7	60.4	57.8
28	54.3	63.7	66.3	64.1	66.5
29	25.6	85.4	79.6	90.0	82.9
30	49.1	86.8	84.1	88.9	84.7

[a] The relative energies with zero-point energy correction

[b] Isomer **1** is 0.5 kcal/mol lower in energy than isomer **2** at the CCSD (T)/ 6-311++G (3df,2pd) level. Based on MP2-optimized structures, isomer **1** is 6.3 and 0.9 kcal/mol lower in energy than isomer **2** at the MP2/6-311++G and CCSD(T)/6-311++G(3df,2pd) levels, respectively

[c] The total energies of reference isomer **1** at the B3LYP/6-311+G(d) level is -188.6113084 a.u., at QCISD/6-311+G(d) level is -188.040286 a.u., at QCISD(T)/6-311+G(d) level is -188.0828547 a.u., at CCSD/6-311+G(d) level is -188.0378136 a.u., at CCSD /6-311+G(d) level is -188.0811976 a.u. and at CCSD(T)/6-311++G(3df,2pd) level is -188.1827064 a.u. The total energies of reference isomer **1** at MP2/6-311+G(d) and CCSD(T)/6-311++G(3df,2pd) levels are -187.4149338 and -188.181754 a.u.

are no reports on neutral C_3B_3. In the current work, we carried out a systematic theoretical study to explore the structures, stability, and potential energy surface of planar C_3B_3. It was interesting to find that the structure and bonding features of low-lying isomers of planar C_3B_3 are similar to those of B_6, C_2B_4, and CB_5 clusters. Isomers **1**, **2**, **3**, **4**, **7**, **9**, **12**, **17**, **19**, and **20** of C_3B_3 are stable, both thermodynamically and kinetically, at the B3LYP/6-311+G(d)// CCSD(T)/6-311+G(d) level, and are detectable in the laboratory.

Computational details

First, the geometries of possible planar C_3B_3 isomers (~450) were optimized at the B3LYP [46, 47] /6-31G(d) level and about 100 stable isomers were obtained. Then, 30 low-energy isomers of C_3B_3 were further optimized at the B3LYP/6-311+G(d) level. Vibrational frequency analysis was performed to confirm whether the optimized structures are stable at the same level. Their corresponding transition states were searched for lower-energy isomers **1**–**20** at the B3LYP/6-311+G(d) level. The energies of 30 isomers of C_3B_3 and 22 transition states were calibrated at the QCISD (T) [48] /6-311+G(d) and CCSD(T) [48] /6-311+G(d) levels. For 22 transition states, intrinsic reaction coordinate (IRC) calculations were performed at the B3LYP/6-311+G (d) level to examine whether they connect the related isomers. On the other hand, we carried out natural bond orbital (NBO) [49] analysis on the isomers of C_3B_3 at the B3LYP/6-311+G(d) level. All calculations were carried out using the GAUSSIAN 09 program package [50].

Results and discussion

Structures and potential-energy surface of C_3B_3

The optimized structures of 30 low-lying isomers of C_3B_3 and 22 transition states are represented in Figs. 1 and 2, respectively, in order of energy increase. The structures of possible dissociation fragments are displayed in Fig. 3. The 30 isomers correspond to the local minima in potential energy surface (PES). The relative energies at different levels of theory are listed in Table 1. They can be divided into four categories, including belt-like, fan-like, a ring with exocyclic chain, and chain-like species. For convenience, Arabic numbers are used to represent these isomers. In addition, since the B3LYP/6-311+G(d) calculations demonstrate that the quartet structures are all higher in energy than the corresponding doublet ones, for simplicity the details will not be displayed and discussed here.

As shown in Fig. 1 and Table 1, there are two nearly isoenergetic isomers **1** and **2** obtained at the B3LYP/6-311+G(d)//CCSD(T)/ 6-311+G(d) level, isomer **1** (C_s, $^2A'$), a planar polycyclic geometry composed of one CCB three-membered ring and three BBC three-membered rings, isomer **2** (C_s, $^2A'$), a planar six-membered ring structure including one CCB three-membered ring, one CBBB four-

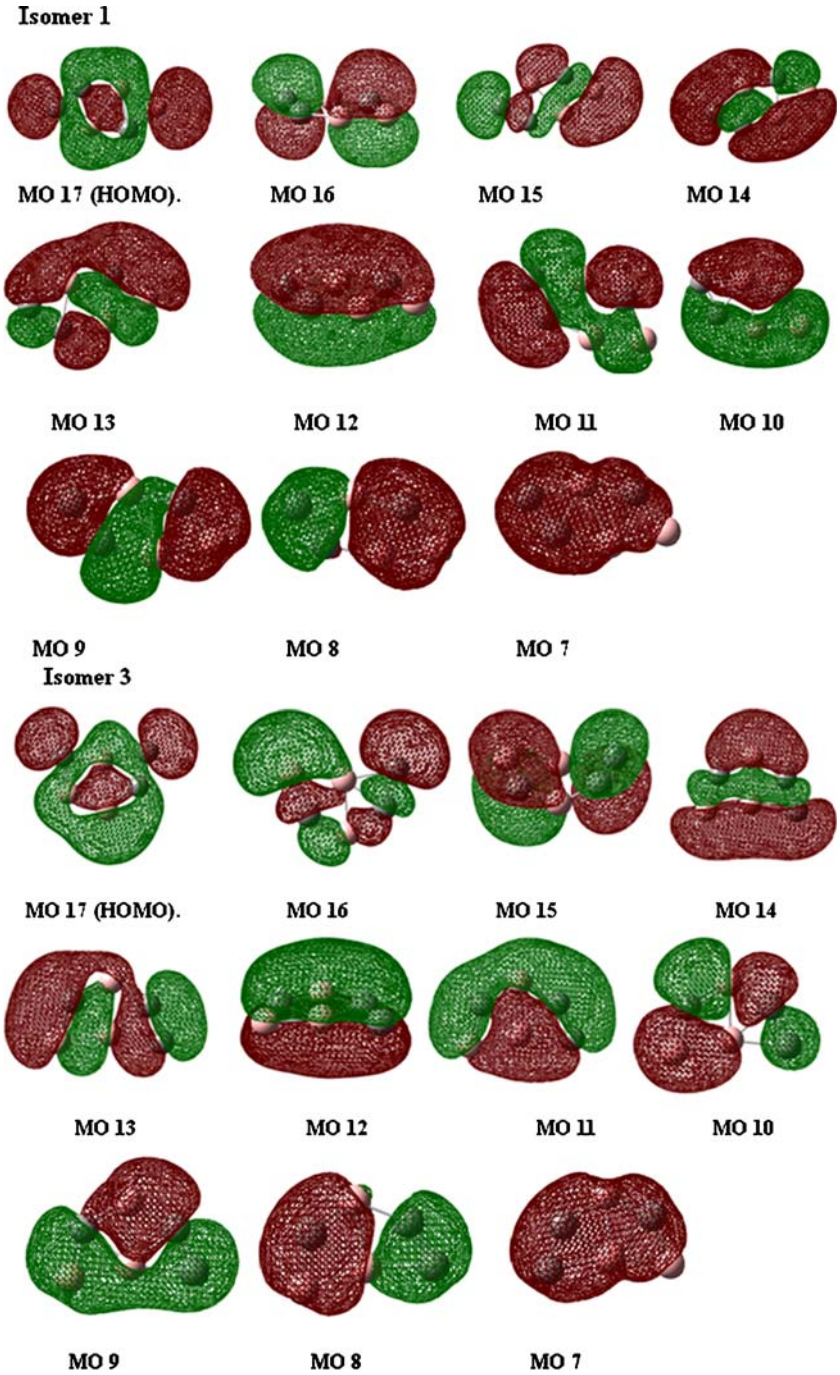

Fig. 4 Valence molecular orbitals (MOs) of isomers **1**, **3**, **6**, and **20** of C_3B_3 at the B3LYP/6-311+G(d) level of theory

membered ring, and one BBC three-membered ring. As shown in Table 1, isomer **2** is 0.2 kcal mol^{-1} higher than isomer **1** at the CCSD(T)/6-311+G(d) level. Moreover, at the CCSD(T)/ 6-311++G(3df, 2pd) level, isomer **1** is 0.5 kcal mol^{-1} lower in energy than isomer **2**. To find the lowest-energy isomer, optimizations on isomers 1 and 2 were performed at the MP2/6-311+G(d) level and the total energies calibrated at the CCSD(T)/6-311++G(3df,2pd) level. The results demonstrate that isomer **1** is 6.3 and 0.9 kcal mol^{-1} lower in energy than isomer **2** at the MP2/6-311++G and CCSD(T) /6-311++G(3df,2pd) levels, respectively. This suggests that both isomer **1** and isomer **2** are possible lowest-energy structures for planar C_3B_3. NBO analysis revealed that the average Wiberg bond indices (WBI) [51] of bonds between circumjacent carbon and boron atoms in isomer **1** is 1.55, revealing that the delocalized π electron in the molecular plane plays an important role in stabilizing the belt-like structure, which is

Fig. 4 (continued)

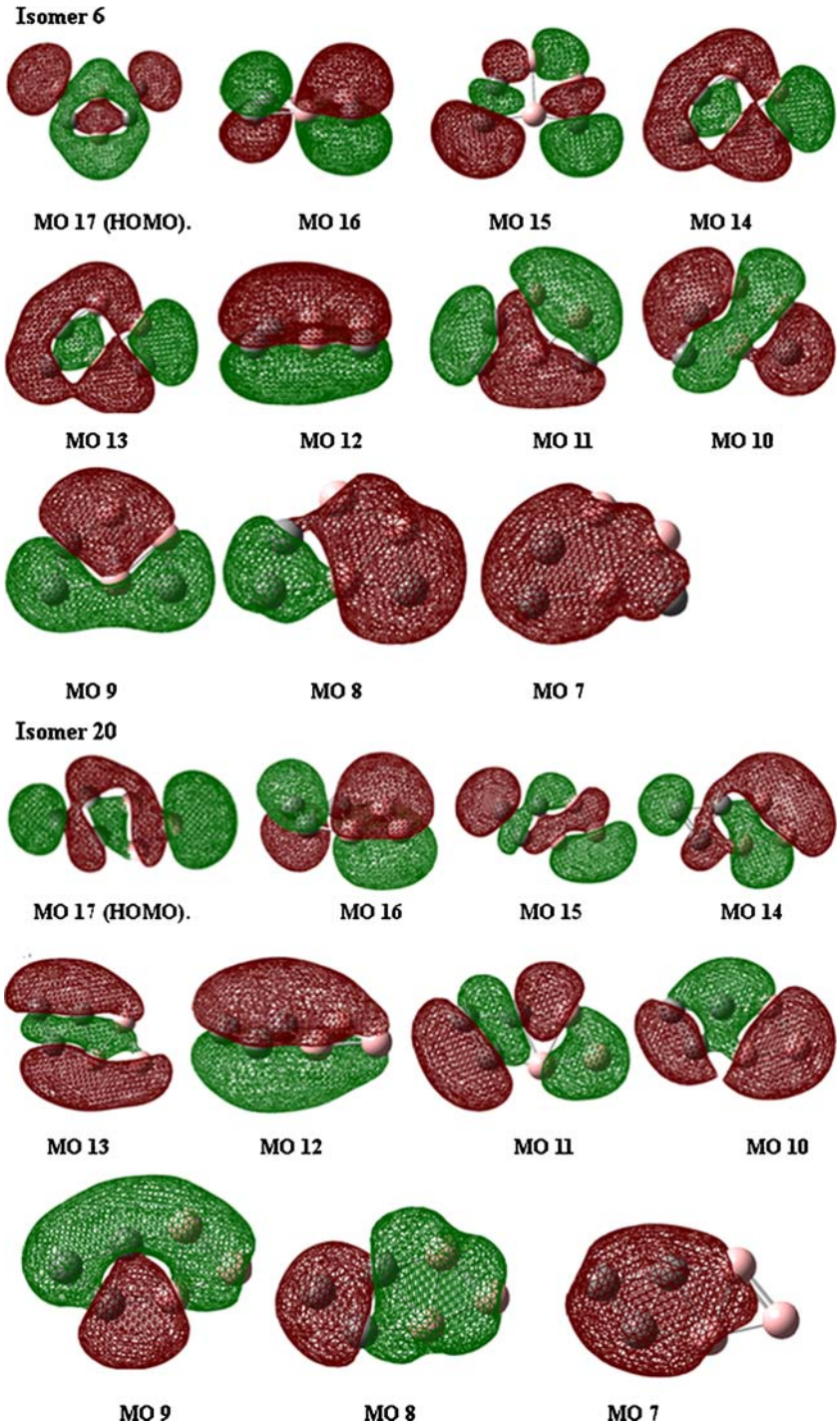

supported by the MO 12 of isomer **1** in Fig. 4. The structure of isomer **20** (C_s, $^2A'$) is similar to that of isomer **1**. Isomer **20** includes one CCC three-membered ring and one BBB three-membered ring and is 45.5 kcal mol^{-1} higher than isomer **1**, which suggests that C_3 and B_3 units are not favorable to the energy of isomer **20**. The average WBI of bonds between circumjacent carbon and boron atoms in isomer **20** is 1.46, suggesting that the π electrons are delocalized in the atom plane, which is in agreement with MO 12 of isomer **20** in Fig. 4. Isomers **4**, **9** and **14** have similar structures with one four-membered ring and two three-membered rings. Isomers **4** and **9** can be obtained by adding one carbon and one boron to two sides of the BBCC four-membered ring. They are 16.06 and 27.59 kcal mol^{-1} higher than isomer **1**, respectively. Isomers **10** and **21** have a planar six-membered ring structure containing one five-membered ring and one BBC three-membered ring. Isomers **10** and **21** are regular six-membered rings. Isomer **10** and

Table 2 Relative energies (kcal mol^{-1}) of transition states at different levels of theory with 6-311+G(d) basis set[a]

System	B3LYP[b]	QCISD	QCISD(T)	CCSD	CCSD(T)
TS5/6	19.4	20.7	20.6	21.1	20.9
TS1/3	25.6	24.9	24.2	25.4	24.3
TS8/11	23.5	26.1	25.8	26.7	26.2
TS1/15	34.0	37.1	36.6	37.1	36.7
TS3/15	33.9	37.6	37.0	37.7	37.2
TS2/11	41.9	43.1	41.0	43.4	41.4
TS2/7	49.3	45.3	45.1	45.8	45.4
TS8/18	41.9	47.8	45.6	49.1	46.6
TS1/13	48.2	48.8	46.7	49.0	46.7
TS12/16	49.3	50.1	48.3	50.6	48.8
TS2/3	47.5	53.4	47.9	55.7	49.8
TS2/8	55.4	61.5	56.9	62.8	57.8
TS2/6	84.7	61.3	56.4	62.7	57.9
TS9/25	56.7	60.2	57.8	60.4	58.1
TS8/19	60.8	70.6	66.9	66.6	64.0
TS2/7*	69.4	67.8	66.3	68.4	66.9
TS16/20	68.0	72.8	67.8	74.6	69.0
TS9/13	69.2	71.0	69.8	71.8	70.0
TS1/9	73.0	74.4	72.7	75.0	73.1
TS2/4	103.3	76.0	75.6	76.3	75.8
TS12/20	73.2	79.8	74.9	82.0	76.1
TS4/17	59.3	79.9	77.0	80.5	77.5

[a] The total energies of reference isomer **1** at different levels of theory are displayed in 'footnote c of Table 1

[b] The relative energies with zero-point energy correction

21 can be formed by breaking the inner C–C bonds of isomers **4** and **14**, respectively. Isomer **12** can be obtained by breaking two inner B–C bonds in the six-membered ring of isomer **9**, with 8.75 kcal mol^{-1} above isomer **9**. In fact, the geometries of isomers **1**, **2**, **4**, **9**, **10**, **12**, **14**, **20**, and **21** can be approximately considered as belt-like structures.

Isomers **3** and **6** are planar six–membered rings involving four three-membered rings. Isomers **3** and **6** are 9.4 and 19.6 kcal mol^{-1} higher than isomer **1**, respectively. Isomers **3** and **6** exhibit a fan-like structure with a planar pentacoordinate boron [52], which follows the octet rule because the total WBI for the pentacoordinate boron are 4.13 and 4.01, respectively. For isomer **3**, the average WBI of bonds between circumjacent boron atoms is 1.50, illustrating that there is a delocalized π bond in the atom plane, which is consistent with the MO 12 of isomer **3** in Fig. 4. The average WBI of the five bonds between the central B atom and the five surrounding atoms is 0.83, indicating the existence of multicentered σ bonds as shown in Fig. 4 (isomer **3**, MO 7). This reveals that the multicentered σ MOs and delocalized π MOs play an important role in formation of isomer **3**. Isomer **6** has a similar bonding character. The structures of isomers **23** and **25** are similar to the structure of isomer **3**. However, they exhibit C_2 symmetry with the ^{2}A state. If they are under the constraint of planar C_{2v} symmetry, isomers **23** and **25** have one and two imaginary frequencies, respectively, at the B3LYP/6-311+G(d) level. The structure of isomer **5** is similar to that of isomer **3** and two inner C–B bonds are broken in isomer **5**.

Isomer **13** contains one three-membered ring and one exocyclic CBCC linear chain. Isomers **18**, **19**, **27**, **28**, and **30** possess similar structures with one four-membered ring and one exocyclic three-atom chain. Isomers **15**, **16**, **17**, **22**, and **24** have analogous geometries. They possess one five-membered ring and one exocyclic C–B or C–C bond. Among them, isomers **15**, **17**, and **22** are 41.5, 27.4, and 7.4 kcal mol^{-1} higher than isomers **1**, **4**, and **14**, respectively. It is noted that isomer **9** can be obtained by moving an exocyclic carbon atom of isomer **16** and is 15.2 kcal mol^{-1} lower than isomer **16**.

Isomers **7**, **8**, **11**, **26** and **29** have chain-like geometrical structures, whereas isomers **11**, **26**, and **29** exhibit linear geometry. Isomers **7** and **8** are more favorable in energy than linear isomers **11**, **26** and **29**.

The geometrical structures of 22 transition states are shown in Fig. 2, and their relative energies at different levels are listed in Table 2. The schematic PES of C_3B_3 clusters is represented in Fig. 5. In order to examine the kinetic stability, various isomerization and dissociation pathways are computed for low-lying 20 isomers of C_3B_3. Since the relative energies of all possible dissociation products are slightly high compared to isomer **1** (>111 kcal mol^{-1} at the B3LYP/6-311+G(d)//CCSD(T)/6-311+G(d) level as displayed in Table 3), the dissociation transition states are not explored.

From Fig. 5, it is easy to see that most isomers have transition states. Moreover, most isomers can be converted into the lower-energy isomers through direct or indirect conversion processes. Because the kinetic stability of an isomer is controlled by the smallest barrier energy, isomers **1** (24.3 kcal mol^{-1} for **1→3** conversion), **2** (45.2 kcal mol^{-1} for **2→7** conversion), **3** (14.9 kcal mol^{-1} for **3→1** conversion), **4** (59.7 kcal mol^{-1} for **4→2** conversion), **7** (19.0 kcal mol^{-1} for **7→2** conversion), **9** (30.5 kcal mol^{-1} for **9→25** conversion), **12** (12.5 kcal mol^{-1} for **12→16** conversion), **17** (34.0 kcal mol^{-1} for 17→**4** conversion), **19** (19.5 kcal mol^{-1} for **19→8** conversion), and **20** (13.6 kcal mol^{-1} for **20→16** conversion) have higher kinetic stability as shown in Fig. 5. It is obvious that isomer **4** is the most stable kinetically, although it is 16.1 kcal mol^{-1} above the most stable isomer **1** thermodynamically. Despite the small difference of 0.2 kcal mol^{-1}at the CCSD(T)/6-311+G(d) level, isomer **2** needs large excess energy of 49.8 kcal mol^{-1} to convert it into isomer **1** via isomer **3**, i.e., **2→3→1**. It is interesting to note that isomer **7** can be converted into isomer

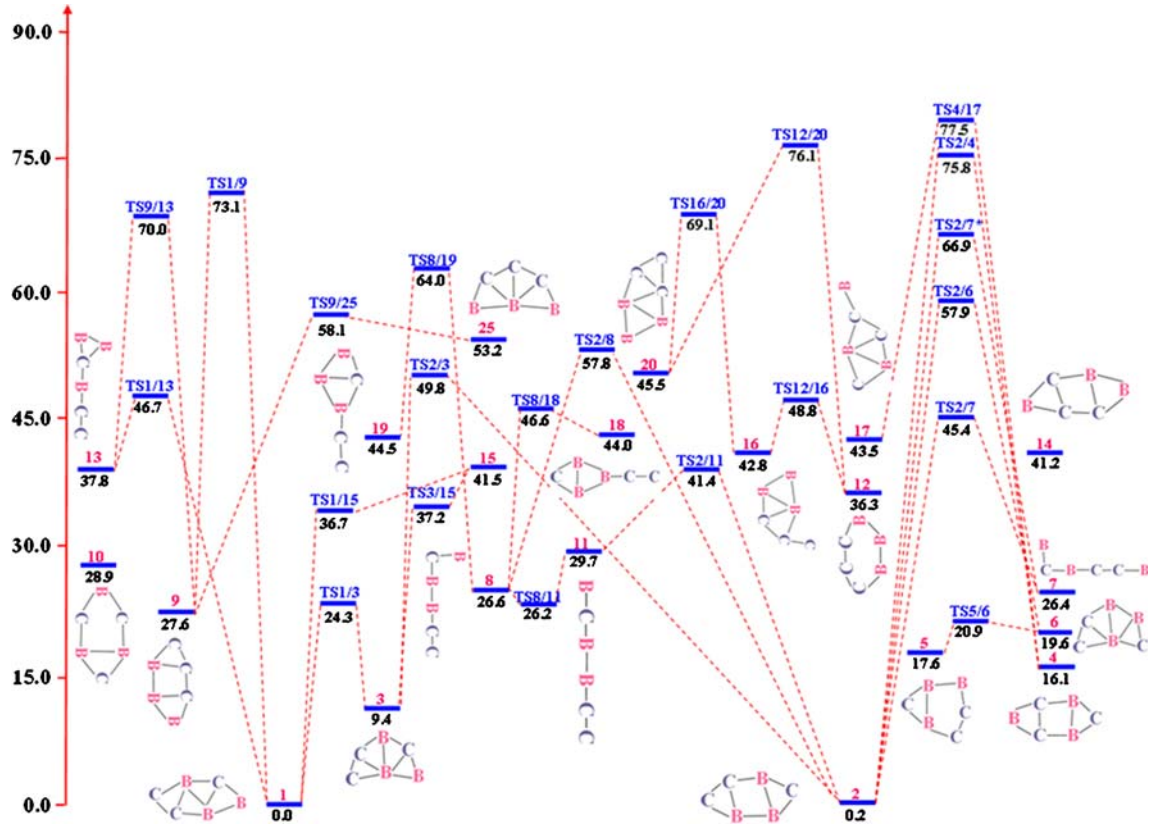

Fig. 5 Schematic potential energy surface (PES) of planar C_3B_3 at the B3LYP/ 6-311+G(d)//CCSD/6-311+G(d) level

2 through two isomerization channels with energy barriers of 19.0 and 40.5 kcal mol^{-1}, respectively. Isomer **12** has the least kinetic stability of all. It can be noted from Table 1 and Fig. 5 that ten isomers (**1**, **2**, **3**, **4**, **7**, **9**, **12**, **17**, **19** and **20**) are stable both thermodynamically and kinetically. It can be expected that these species are detectable in the laboratory. Thus, their vibrational frequencies, infrared intensities, dipoles, rotational constants, and HOMO−LUMO energy gaps are presented in Table 4, which is helpful for future experimental studies.

As shown in Fig. 5, some isomers have a lower conversion barrier of isomerization, e.g., isomer **5** (3.3 kcal mol^{-1}, **5→6**), **6** (1.3 kcal mol^{-1}, **6→5**), **8** (−0.4 kcal mol^{-1}, **8→11**), **11** (−3.5 kcal mol^{-1}, **11→8**), **13** (8.9 kcal mol^{-1}, **13→1**), **15** (−4.3 kcal mol^{-1}, **15→1**), **16** (6.0 kcal mol^{-1}, **16→12**), and **18** (2.6 kcal mol^{-1}, **18→8**). Clearly, these high-energy isomers are kinetically unstable. It is noted that no transition states connecting isomer **10** or **14** can be located from our calculations. As mentioned above, isomer **10** can be obtained by breaking the inner C–C bond of isomer **4**. However, the transition state between isomers 4 and 10 was not located. A similar situation exists for isomers **9** and **12**.

Properties of the most relevant isomers

To obtain a more accurate energy order, the single point energies of the most relevant isomers, i.e., isomers **1**, **2**, **3**, **4**, **7**, **9**, **12**, **17**, **19**, and **20**, were calculated at different levels involving B3LYP, QCISD, QCISD(T), CCSD and CCSD(T) methods with the 6-311+G(d) basis set as shown in Table 1. It should be noted from Table 1 that the relative energy order is same for B3LYP, QCI, and CC methods except for isomers **7** and **9**. In fact, isomer **7** is 2.4 kcal mol^{-1} higher than isomer 9 at the B3LYP/6-311+G(d) level and the energy order is changed if QCI and CC methods with electron correlation are used.

The valence MOs of some of the isomers are shown in Fig. 4. As mentioned above, for low-energy isomers of C_3B_3, there are multicentered σ MOs, delocalized σ MOs, and delocalized π MOs. For simplicity, we describe the valence MOs of isomer 1 as an example. The MO 17, the highest occupied molecular orbital (HOMO) with one electron, is a σ molecular orbital with four-center bonding among the middle four atoms of isomer **1**. It is clear that MOs 7, 8, and 9 also are σ molecular orbitals with multicenter bonding. MOs 12 and 16 are delocalzied π molecular orbitals. The remaining orbitals are all delocalzied σ molecular orbitals. The core MOs (MO 1–5) are not represented in Fig. 4. Therefore, the delocalized σ MOs, multi-centered σ MOs, and delocalized π MOs play an important role in stabilizing the structures of isomer **1**. It was noted that isomers **1**, **2**, **3**, **4**, **7**, **9**, **12**, **17**, **19** and **20** have similar bonding character, which is also consistent

Table 3 Relative energies of the dissociation fragments of the C_3B_3 isomers at the B3LYP/6-311+G(d) and CCSD(T)/6-311+G(d) levels[a]

c	B3LYP[b] (kcal/mol)	CCSD(T)[b] (kcal/mol)	Species	B3LYP[b] (kcal/mol)	CCSD(T)[b] (kcal/mol)
cCBBCB($^2A_2$) + C(^3P)	162.4	157.1	cCBB ($^1A_1$) + CCB($^2\Sigma$)	134.5	126.3
cCBCBB($^2A''$) + C(^3P)	172.0	178.0	BCB ($^3\Sigma_u$) + CCB($^2\Sigma$)	142.7	149.4
cCCBBB($^2A''$) + C(^3P)	178.1	168.3	BCB($^1\Sigma_g$) + cCCB($^2A'$)	169.7	131.5
cCBCBB($^2A'$) + C(^3P)	180.6	174.8	cCBB ($^1A_1$) + cCCB($^2A'$)	132.6	119.5
cBCCBB($^4B_1$) + C(^3P)	182.3	176.5	BCB ($^3\Sigma_u$) + cCCB($^2A'$)	140.8	142.7
cCBCBB($^4A''$) + C(^3P)	182.6	178.2	cCBCCB ($^1A'$) + B(^2P)	131.4	119.3
cBCBC ($^3B_{1u}$) + CB($^2\Pi$)	175.0	172.6	BCCCB ($^3\Sigma_u$) + B(^2P)	141.2	146.4
cCBBC($^3A'$) + CB($^2\Pi$)	181.3	179.3	BCBCC($^3A'$) + B(^2P)	142.8	150.6
BCCB ($^1\Sigma_g$) + CB($^2\Pi$)	193.0	180.5	BCBCC($^3\Sigma$) + B(^2P)	143.0	155.9
cBCBC ($^3B_{1u}$) + CB($^4\Sigma$)	200.3	184.3	CCCB($^4\Sigma$) + BB($^1\Sigma_g$)	221.8	214.4
cCBBC($^3A'$) + CB($^4\Sigma$)	206.6	191.0	cCCBC($^2A_1$) + BB($^1\Sigma_g$)	222.0	203.0
BCCB ($^1\Sigma_g$) + CB($^4\Sigma$)	218.2	192.2	cCBCC($^2A_1$) + BB($^1\Sigma_g$)	228.6	212.6
cBBBC($^2B_2$) + CC($^3\Sigma_g$)	183.5	172.8	CCCB($^4\Sigma$) + BB($^3\Sigma_g$)	201.0	197.6
cCBBB($^2A_1$) + CC($^3\Sigma_g$)	187.8	176.0	cCCBC($^2A_1$) + BB($^3\Sigma_g$)	201.2	186.3
cBBBC($^4A'$) + CC($^3\Sigma_g$)	209.9	196.5	cCBCC($^2A_1$) + BB($^3\Sigma_g$)	207.8	195.9
BCBB($^2\Sigma$) + CC($^3\Sigma_g$)	214.6	111.8	cCCCBB ($^1A'$) + B(^2P)	152.0	138.0
cBBBC($^2B_2$) + CC($^1\Sigma_g$)	210.6	180.7	cCBBCC ($^1A_1$) + B(^2P)	153.9	142.1
cCBBB($^2A_1$) + CC($^1\Sigma_g$)	215.0	183.8	BBB($^2\Sigma_g$) + CCC($^1\Sigma_g$)	202.0	224.8
cBBBC($^4A'$) + CC($^1\Sigma_g$)	237.0	204.3	cBBB($^2A_1'$) + CCC($^1\Sigma_g$)	157.9	152.0
BCBB($^2\Sigma$) + CC($^1\Sigma_g$)	241.7	119.7	BBB($^2\Sigma_g$) + CCC($^3A_1'$)	221.7	245.1
BCB($^1\Sigma_g$) + CCB($^2\Sigma$)	171.6	138.3	cBBB($^2A_1'$) + CCC($^3A_1'$)	177.5	172.3

[a] The total energies of reference isomer **1** at different levels of theory are displayed in 'footnote c of Table 1

[b] The basis set is 6-311+G(d) for B3LYP and CCSD(T)

with the results from C_4B [43], CB_4 [44] and B_6 [50] isomers.

As mentioned above, the lowest-energy structures of C_3B_3 (isomers **1** and **2**) are stable both thermodynamically and kinetically. We also used three criteria suggested by Hoffmann [53] to examine the chemical viability of isomers **1** and **2** of C_3B_3. Firstly, as shown in Table 4, the HOMO−LUMO energy gaps of isomers **1** and **2** are relatively larger (~10 eV), which reveals that they have higher stability. Secondly, the calculated smallest vibrational frequencies of isomers **1** and **2** are 195 and 246 cm^{-1} at the B3LYP/6-311+G(d) level, respectively, as represented in Table 4, which are reasonably large. Thirdly, the dissociation reaction energies (DEs) were computed at the CCSD(T)/6-311+G(d) level based on the following reactions:

$$C_3B_3 \rightarrow C_3B + B_2 \qquad DE = 186.3\ kcal \cdot mol^{-1} \qquad (1)$$

$$C_3B_3 \rightarrow C_2B_2 + CB \qquad DE = 172.6\ kcal \cdot mol^{-1} \qquad (2)$$

$$C_3B_3 \rightarrow C_2B_2 + 1/2C_2 + 1/2B_2 \qquad DE = 171.2\ kcal \cdot mol^{-1} \qquad (3)$$

$$C_3B_3 \rightarrow C_2B + CB_2 \qquad DE = 119.5\ kcal \cdot mol^{-1} \qquad (4)$$

$$C_3B_3 \rightarrow C_2B + 1/2C_2 + B_2 \qquad DE = 235.6\ kcal \cdot mol^{-1} \qquad (5)$$

$$C_3B_3 \rightarrow CB_2 + C_2 + 1/2B_2 \qquad DE = 227.3\ kcal \cdot mol^{-1} \qquad (6)$$

$$C_3B_3 \rightarrow CB_2 + CB + 1/2C_2 \qquad DE = 228.6\ kcal \cdot mol^{-1} \qquad (7)$$

$$C_3B_3 \rightarrow 3/2C_2B_2 \qquad DE = 85.1\ kcal \cdot mol^{-1} \qquad (8)$$

Table 4 Vibrational frequencies (cm^{-1}) and infrared intensities (kcal mol^{-1}; in parentheses), dipole moments (D), rotational constants (GHz), and HOMO−LUMO gaps [ΔE(gap), eV] of the relevant isomers of C_3B_3 at the B3LYP/6-311+G(d) level

Isomer	Frequency (infrared intensity)	Dipole moment	Rotational constant	ΔE (gap)	ΔE (gap) [a]
1	195(10), 438(3), 491(15), 520(26), 598(7), 653(23) 826(9), 961(0), 1061(15), 1274 (18), 1405(14), 1704(110)	1.0473	18.85907 4.27626 3.48585	3.54	10.15
2	246(25), 332(7), 449(3), 491(5), 660(7), 750(37), 758(32), 943(5), 1100(34), 1418 (70), 1446(59), 1706(21)	0.5085	16.73772 4.36020 3.45910	3.42	10.22
3	227(3), 294(4), 407(8), 507(12), 580(0), 665(4), 717(12), 883(30), 1062(7), 1268 (17), 1502(23), 1724(13)	2.5579	12.94669 4.88638 3.54748	3.37	9.69
4	242(11), 374(15), 466(14), 504(0), 632(4), 770(9), 852(17), 1109(28), 1137(36), 1438(24), 1468(3), 1578(220)	1.5650	17.86041 4.38236 3.51893	3.13	10.43
5	86(16), 236(43), 242(18), 452(14), 460(7), 633(25), 763(19), 830(7), 928(6), 1441 (201), 1558(28), 1804(8)	2.3855	8.90414 5.97221 3.57463	2.62	9.89
6	176(0), 319(17), 420(32), 467(6), 500(5), 620(16), 648(19), 977(8), 1094(6), 1258 (14), 1462(1), 1680(2)	2.9930	11.94560 5.12510 3.58640	2.88	9.52
7	80(12), 92(20), 116(3), 238(5), 245(0), 510(5), 513(11), 615(61), 1044(415), 1464 (29), 1709(601), 2223(233)	2.5963	43.19846 1.62766 1.56855	2.83	9.78
8	83(11), 100(16), 143(2), 238(7), 244(1), 497(4), 499(8), 553(3), 1299(24), 1468(44), 1707(255), 2096(1165)	3.8693	41.18274 1.51295 1.45934	4.19	10.30
9	246(25), 332(7), 449(3), 491(5), 660(7), 750(37), 758(32), 943(5), 1100(34), 1418 (70), 1446(59), 1706(21)	1.0787	16.97835 4.47010 3.53848	2.68	9.34
10	218(5), 360(11), 418(0), 433(12), 537(36), 672(31), 824(6), 968(13), 1291(11), 1435 (222), 1491(5), 1502(0)	2.0631	13.91179 4.94820 3.64997	2.58	8.10
11	74(2), 74(2), 145(11), 145(11), 278(19), 278(19), 492(0), 499(0), 499(0), 1182(2), 1414(72), 1960(1524)	5.2332	1.240984	3.84	10.21
12	215(1), 280(0), 383(31), 399(0), 439(22), 664(48), 819(12), 1026(4), 1160(15), 1288 (16), 1581(11), 1790(289)	1.0817	13.07328 5.07299 3.65478	2.04	7.98
13	91(5), 106(5), 189(1), 232(0), 464(6), 520(34), 582(24), 718(69), 1109(30), 1340 (10), 1690(53), 2093(1573)	5.2961	34.80168 1.80816 1.71885	3.25	10.47
14	122(4), 389(5), 423(3), 461(2), 597(2), 730(14), 876(7), 945(25), 1111(9), 1331(52), 1398(15), 1553(3)	0.5727	18.98873 4.43527 3.59546	2.77	10.38
15	150(4), 152(7), 326(12), 509(11), 561(134), 605(451), 712(146), 847(245), 969(68), 1194(8), 1401(337),519(1655)	1.7648	19.52372 3.40903 2.90226	3.35	7.59
16	212(0), 272(3), 288(12), 472(0), 568(3), 620(11), 708(5), 905(39), 1034(16), 1212 (26), 1095(27), 1755(78)	2.5985	13.36906 4.61248 3.42933	2.96	9.67
17	117(9), 161(17), 321(20), 483(2), 527(12), 693(4), 720(98), 890(20), 1192(55), 1442 (5), 1667(537)	2.1742	19.76512 3.38233 2.88810	2.66	8.22
18	34(49), 119(15), 141(6), 257(6), 500(1), 532(1), 571(3), 882(0), 1208(24), 1340(10), 1485(11), 1921(335)	2.4380	34.29599 2.14248 2.01651	3.77	10.44
19	95(25), 126(4), 259(0), 334(6), 444(60), 490(11), 608(15), 877(0), 1033(38), 1320 (15), 1509(5), 1897(171)	4.7356	35.49118 2.20391 2.07505	3.52	9.00
20	181(11), 437(0), 455(28), 472(0), 514(0), 645(5), 800(0), 953(34), 1038(3), 1194 (14), 1248(4), 1598(9)	1.4054	18.81643 4.25309 3.46899	3.36	9.72

[a] HOMO−LUMO gaps(eV) at the CCSD/6-311+G(d) level

$$C_3B_3 \rightarrow 3CB \qquad DE = 347.5\ kcal \cdot mol^{-1} \qquad (9)$$

$$C_3B_3 \rightarrow 3C + 3B \qquad DE = 628.6\ kcal \cdot mol^{-1} \qquad (10)$$

In the above reactions, the most stable states for C_3B_3, C_3B, C_2B_2, C_2B, CB_2, CB, B_2, C_2, C, and B were used. It is not difficult to see that all the reactions mentioned above are quite endothermic for the dissociation of C_3B_3 since their DEs are relatively large positive values (>85 kcal mol^{-1}). Therefore, isomers **1** and **2** of C_3B_3 have high stability according to Hoffmann's criteria.

Comparison of boron-doped carbon clusters

From previous studies of C_nB_m $(n + m = 6)$ [33–37, 43–45] clusters, it was found that the geometry of isomer **1** of the C_3B_3 cluster is similar to the structure of the second-lowest isomer of the CB_5 cluster [36, 45], when two boron atoms are replaced by two carbon atoms. The geometry of

isomer **2** of the C_3B_3 cluster is similar to the most stable structures of both the C_2B_4 cluster [33, 35, 37] and a pure B_6 [54] cluster. Meanwhile, the pattern of isomer **3** for C_3B_3 clusters shares similarity with the third low-lying structures of B_6 [55] clusters. It is well known that, for C_4B_2 [33] and C_5B [34, 45] clusters, the two lowest-energy structures are chains or monocyclic shapes, which have a tendency to form the structures of pure C_6 [55] clusters. However, it is noteworthy that the structural features of the low-lying structures for C_3B_3 clusters are similar to those of B_6 [53] clusters, just like C_2B_4 [33, 35, 37] and CB_5 [34, 45] clusters.

Conclusions

We have obtained optimized structures of 30 low-energy isomers of C_3B_3 at the B3LYP/6-311+G(d) level, PES of low-energy isomers **1**–**20** of C_3B_3 at the CCSD(T)/6-311 +G(d) level ,and some physical properties. C_3B_3 exhibits several interesting features: (1) the lowest-energy structures of C_3B_3 include isomers **1** and **2**, which are nearly isoenergetic at the B3LYP/6-311+G(d), CCSD(T)/6-311 +G(d), and CCSD(T)/6-311++G (3df,2pd) levels; (2) the geometry characters of low-lying isomers for planar C_3B_3 are similar to those of B_6, C_2B_4, and CB_5 clusters; (3) NBO analyses demonstrate that the delocalized σ MOs, multi-centered σ MOs, and delocalized π MOs play an important role in stabilizing structures of low-energy isomers of C_3B_3; (4) the 10 isomers **1**, **2**, **3**, **4**, **7**, **9**, **12**, **17**, **19**, and **20** of C_3B_3 are stable both thermodynamically and kinetically, which suggests that these isomers will be detectable in the laboratory in future; (5) the PES of C_3B_3 is complicated and interesting. In particular, isomer **7** can be converted into **2** via two isomerization channels with energy barriers of 19.0 and 40.5 kcal mol^{-1}, respectively.

Acknowledgments This work was supported by grants from the National Science Foundation of China (No. 20236010, 20246002, 20376032, 20706029, and 20876073), Jiangsu Science and Technology Department of China (No. BK2008372), and Nanjing University of Technology of China.

References

1. Ho KM, Shvartsburg AA, Pan B, Lu ZY, Wang CZ, Wacker JG, Fye JL, Jarrold MF (1998) Structures of medium-sized silicon clusters. Nature 392(6676):582–585
2. Raghavachari K, Rohlfing CM (1992) Structures of Si_{10}. Are there conventionally bonded low-energy isomers? Chem Phys Lett 198(5):521–525
3. Asmis KR, Taylor TR, Neumark DM (1999) Electronic structure of indium phosphide clusters: anion photoelectron spectroscopy of $In_xP_x^-$ and $In_{x+1}P_x^-(x = 1 - 13)$ clusters. Chem Phys Lett 308(5–6):347–354
4. Yoo S, Zeng XC, Zhu XL, Bai J (2003) Possible lowest-energy geometry of silicon clusters Si_{21} and Si_{25}. J Am Chem Soc 125 (44):13318–13319
5. Yoo S, Zhao JJ, Wang JL, Zeng XC (2004) Endohedral silicon fullerenes Si_N ($27 \le N \le 39$). J Am Chem Soc 126(42):13845–13849
6. Bai J, Cui LF, Wang JL, Yoo S, Li X, Jellinek J, Koehler C, Frauenheim T, Wang LS, Zeng XC (2006) Structural evolution of anionic silicon clusters Si_N^- ($20 \le N \le 45$). J Phys Chem A 110 (3):908–912
7. Balasubramanian K, Zhu XL (2001) Spectroscopic properties of mixed gallium arsenide tetramers: $GaAs^{\pm}$, $GaAs_3$, $Ga_3As^{\pm}$, and Ga_3As. J Chem Phys 115(19):8858–8867
8. Cao ZJ, Balasubramanian K (2007) Unusual geometries and spectroscopic properties of electronic states of In_2N_2. Chem Phys Lett 439(4–6):288–295
9. Zhu XL (2003) Spectroscopic properties for Al_2As, $AlAs_2$, and their ions. Theochem 638(1–3):99–105
10. Zhu XL, Zhou ZH (2004) Electronic states for Al_2As_2 and its ions. Theochem 671(1–3):105–109
11. Zhu XL (2005) Spectroscopic properties of gallium arsenide tetramers: Ga_2As_2, $Ga_2As_2^+$ and $Ga_2As_2^-$. Spectrochim Acta A 61 (11–12):2730–2736
12. Zhu XL, Zeng XC (2003) Structures and stabilities of small silicon clusters: ab initio molecular-orbital calculations of Si_7-Si_{11}. J Chem Phys 118(11–12):3558–3570
13. Zhu XL, Zeng XC, Lei YA, Pan BJ (2004) Structures and stability of medium silicon clusters. II. Ab initio molecular orbital calculations of Si_{12}-Si_{20}. Chem Phys 120(19):8985–8995
14. Zhu XL, Lu XH, Feng X (2007) Geometries and electronic structures of metastable C_2N_4 and its ions. Spectrochim Acta A 67 (3–4):756–761
15. Zhu XL (2007) Theoretical study of electronic structures and spectroscopic properties of Ga_3Sn, $GaSn_3$, and their ions. Spectrochim Acta A 66(1):153–162
16. Zhu XL (2007) Jahn-Teller distortion geometries and electronic structures of Ga_3Ge, $GaGe_3$, and their ions. Spectrochim Acta A 66(2):512–520
17. Zhu XL (2005) Electronic states of Ga_3Si, $GaSi_3$, and their ions. Spectrochim Acta A 62(1–3):596–603
18. Zhang D, Mcllroy DN, Geng Y, Norton MG (1999) Growth and characterization of boron carbide nanowires. J Mater Sci Lett 18 (5):349–351
19. Bao L, Li C, Tian Y, Tian J, Hui C, Wang X, Shen C, Gao H (2008) Synthesis and photoluminescence property of boron carbide nanowires. Chin Phys B 17(12):4585–4591
20. Mcllroy DN, Zhang D, Kranov Y, Norton MG (2001) Nano-springs. Appl Phys Lett 79(10):1540–1542
21. Xu F, Bando Y (2004) Formation of two-dimensional nano-materials of boron carbides. J Phys Chem B 108(23):7651–7655
22. Pender MJ, Sneddon LG (2000) An efficient template synthesis of aligned boron carbide nanofibers using a single-source molecular precursor. Chem Mater 12(2):280–283
23. Kaminaga F, Sato S, Okamoto Y (1992) Evaluation of gap heat transfer between boron carbide pellet and cladding in control rod of FBR. J Nucl Sci Technol 29(2):121–130
24. Swinyard BM (1991) Atomic oxygen protection of carbon and polycarbonate using boron carbide coating. J Spacecr Rockets 28 (6):730–733
25. Knight LB Jr, Cobranchi ST, Petty JT, Earl E, Feller D, Davidson ER (1989) Electron spin resonance investigations of $^{11}B^{12}C$, $^{11}B^{13}C$, and $^{10}B^{12}C$ in neon, argon, and krypton matrices at 4 K: Comparison with theoretical results. J Chem Phys 90(2):690–699

26. Presilla-Marquez JD, Larson CW, Carrick PG, Rittby CML (1996) Fourier transform infrared spectroscopy of the ν_2 vibration of BC_2 in Ar at 10 K. J Chem Phys 105(9):3398–3405
27. Presilla-Marquez JD, Carrick PG, Larson CW (1999) Vibrational spectra of linear BC_3 and linear B_2C_2 in argon at 10K. J Chem Phys 110(12):5702–5709
28. Wang C, Huang R, Liu Z, Zheng L (1995) C_nB^-(n<13): laser generation and ab initio calculations. Chem Phys Lett 242(3):355–360
29. Yamamoto H, Saito T (2003) Fabrication and stability of binary clusters by reactive molecular ion irradiation. Nucl Instr Methods Phys Res B 206:42–46
30. Becker S, Dietze HJ (1988) Cluster ions in the laser mass spectra of boron carbide. Int J Mass Spectrom Ion Process 82(3):287–298
31. Zhan C, Iwata S (1997) Ab initio studies on the structures, vertical electron detachment energies, and fragmentation energies of C_nB^- clusters. J Phys Chem A 101(4):591–596
32. Pascoli G, Lavendy H (2002) Magic numbers in heteroatom-containing carbon monocycles. Eur Phys J D 19(3):339–348
33. Wang L, Zhang C, Wu H (2005) Structure, stability and spectra of C_nB^{δ}(δ=0, ±1; n = 1–6). Acta Phys Chim Sin 21(3):244–249
34. Chuchev K, BelBruno JJ (2004) Density functional theory study of the isomers of C_nB and C_nB_2. J Phys Chem A 108(24):5226–5233
35. Shao JL, Zhu XL, Lu XH, Shi RW (2008) Geometries and stabilities of (n+4)-membered monocyclic C_nB_4(n=2–9) clusters. Theochem 855(1–3):82–91
36. Wang R, Zhang D, Zhu R, Liu C (2007) Density functional theory study of B_nC(n=1–7) clusters. Theochem 817(1–3):119–123
37. Wang R, Zhang D, Zhu R, Liu C (2007) Theoretical study of boron-carbon clusters B_nC_2(n=1–6). Acta Chim Sin 65(19):2092–2096
38. Pei Y, Zeng XC (2008) Probing the planar tetra-, penta-, and hexacoordinate carbon in carbon-boron mixed clusters. J Am Chem Soc 130(8):2580–2592
39. Wang Z, PvR S (2001) Construction principles of "hyparenes": families of molecules with planar pentacoordinate carbons. Science 292(5526):2465–2469
40. Exner K, PvR S (2000) Planar hexacoordinate carbon: a viable possibility. Science 290(5498):1937–1940
41. Minyaev RM, Gribanova TN, Starikov AG, Minkin VI (2002) Heptacoordinated carbon and nitrogen in a planar boron ring. Dokl Chem 382(4–6):41–45
42. Minyaev RM, Gribanova TN, Starikov AG, Minkin VI (2001) Octacoordinated main-group element centres in a planar cyclic B8 environment: an ab initio study. Mendeleev Commun 11(6):213–214
43. McAnoy AM, Bowie JH, Blanksby SJ (2003) A theoretical study of C_4B isomers. The interconversion of CCBCC and CCCCB via cyclic C_4B. J Phys Chem A 107(47):10149–10153
44. Liu C, Tang M, Wang H (2007) The conversion among various B_4C clusters: a density functional theoretical study. J Phys Chem A 111(4):704–709
45. Liu C, Liu L, Han P, Tang M, Fu H (2008) Structure and stability of B_5C and C_5B clusters. Rapid Commun Mass Spectrom 22 (22):3599–3607
46. Becke AD (1993) Density-functional thermochemistry. III. The role of exact exchange. J Chem Phys 98(7):5648–5652
47. Lee C, Yang W, Parr RG (1988) Development of the Colle-Salvetti correlation-energy formula into a functional of the electron density. Phys Rev B 37(2):785–789
48. Pople JA, Head-Gordon M, Raghavachari K (1987) Quadratic configuration interaction. A general technique for determining electron correlation energies. J Chem Phys 87(10):5968–5975
49. Reed AE, Curtiss LA, Weinhold F (1988) Intermolecular interactions from a natural bond orbital, donor-acceptor viewpoint. Chem Rev 88(6):899–966
50. Frisch MJ, Trucks GW, Schlegel HB, Scuseria GE, Robb MA, Cheeseman JR, Scalmani G, Barone V, Mennucci B, Petersson GA, Nakatsuji H, Caricato M, Li X, Hratchian HP, Izmaylov AF, Bloino J, Zheng G, Sonnenberg JL, Hada M, Ehara M, Toyota K, Fukuda R, Hasegawa J, Ishida M, Nakajima T, Honda Y, Kitao O, Nakai H, Vreven T, Montgomery JA Jr, Montgomery JA Jr, Peralta JE, Ogliaro F, Bearpark M, Heyd JJ, Brothers E, Kudin KN, Staroverov VN, Kobayashi R, Normand J, Raghavachari K, Rendell A, Burant JC, Iyengar SS, Tomasi J, Cossi M, Rega N, Millam JM, Klene M, Knox JE, Cross JB, Bakken V, Adamo C, Jaramillo J, Gomperts R, Stratmann RE, Yazyev O, Austin AJ, Cammi R, Pomelli C, Ochterski JW, Martin RL, Morokuma K, Zakrzewski VG, Voth GA, Salvador P, Dannenberg JJ, Dapprich S, Daniels AD, Farkas O, Foresman JB, Ortiz JV, Cioslowski J, Fox DJ (2009) Gaussian 09, Rev A.02. Gaussian Inc, Wallingford
51. Wiberg KB (1968) Application of the pople-santry-segal CNDO method to the cyclopropylcarbinyl and cyclobutyl cation and to bicyclobutane. Tetrahedron 24(3):1083–1096
52. Yu H, Sang R, Wu Y (2009) Structure and aromaticity of $B_6H_5^+$ cation: a novel borhydride system containing planar pentacoordinated boron. J Phys Chem A 113(14):3382–3386
53. Hoffmann R, PvR S, Schaefer HF (2008) Predicting molecules - more realism, please! Angew Chem Int Ed 47 (38):7164–7167
54. Ma J, Li Z, Fan K, Zhou M (2003) Density functional theory study of the B_6, B_6^+, B_6^-, and B_6^{2-} clusters. Chem Phys Lett 372 (5–6):708–716
55. Masso H, Senent ML (2009) J Phys Chem A. doi:10.1021/jp902083c